Altered global brain signal in schizophrenia

Genevieve J. Yang[a,b,c,1], John D. Murray[d,1], Grega Repovs[e], Michael W. Cole[f], Aleksandar Savic[a,c,g], Matthew F. Glasser[h], Christopher Pittenger[a,b,c,i], John H. Krystal[a,c,j], Xiao-Jing Wang[d,k], Godfrey D. Pearlson[a,l,m], David C. Glahn[a,m], and Alan Anticevic[a,b,c,i,j,2]

[a]Department of Psychiatry and [l]Department of Neurobiology, Yale University School of Medicine, New Haven, CT 06511; [b]Interdepartmental Neuroscience Program, Yale University, New Haven, CT 06511; [i]Department of Psychology, Yale University, New Haven, CT 06520; [c]Abraham Ribicoff Research Facilities, Connecticut Mental Health Center, New Haven, CT 06519; [d]Center for Neural Science, New York University, New York, NY 06510; [e]Department of Psychology, University of Ljubljana, 1000 Ljubljana, Slovenia; [f]Center for Molecular and Behavioral Neuroscience, Rutgers University, Newark, NJ 07102; [g]University Psychiatric Hospital Vrapce, University of Zagreb, Zagreb 10000, Croatia; [h]Department of Anatomy and Neurobiology, Washington University in St. Louis, MO 63130; [j]National Institute on Alcohol Abuse and Alcoholism Center for the Translational Neuroscience of Alcoholism, New Haven, CT 06519; [k]New York University–East China Normal University Joint Institute of Brain and Cognitive Science, New York University, Shanghai, China; and [m]Olin Neuropsychiatry Research Center, Institute of Living, Hartford Hospital, CT 06106

Edited by Marcus E. Raichle, Washington University in St. Louis, St. Louis, MO, and approved April 7, 2014 (received for review March 22, 2014)

Neuropsychiatric conditions like schizophrenia display a complex neurobiology, which has long been associated with distributed brain dysfunction. However, no investigation has tested whether schizophrenia shows alterations in global brain signal (GS), a signal derived from functional MRI and often discarded as a meaningless baseline in many studies. To evaluate GS alterations associated with schizophrenia, we studied two large chronic patient samples ($n = 90$, $n = 71$), comparing them to healthy subjects ($n = 220$) and patients diagnosed with bipolar disorder ($n = 73$). We identified and replicated increased cortical power and variance in schizophrenia, an effect predictive of symptoms yet obscured by GS removal. Voxel-wise signal variance was also increased in schizophrenia, independent of GS effects. Both findings were absent in bipolar patients, confirming diagnostic specificity. Biologically informed computational modeling of shared and nonshared signal propagation through the brain suggests that these findings may be explained by altered net strength of overall brain connectivity in schizophrenia.

resting-state | global signal | psychiatric illness

The brain of humans and other mammalian species is organized into large-scale systems that exhibit coherent functional relationships across space and time (1). This organizational principle was discovered in the human brain primarily through examination of correlated spontaneous fluctuations in the blood-oxygenation level-dependent (BOLD) signal, which reflects blood flow and is interpreted as a surrogate marker for regional brain metabolic activity (2–4). Such resting-state functional connectivity (rs-fcMRI) analyses further revealed the functional architecture of the brain (1, 3) and its alterations in pathological states, wherein disruptions of brain function may be restricted to certain regions, or extend globally because of widespread neurotransmitter abnormalities (5, 6), possibly affecting widespread global signals (GS) (7).

Schizophrenia (SCZ) has been described as a disorder of distributed brain "dysconnectivity" (8), emerging from complex biological alterations (9) that may involve extensive disturbances in the NMDA glutamate receptor, altering the balance of excitation and inhibition (10). The symptoms of SCZ are correspondingly pervasive (11), leading to a lifetime of disability for most patients (12) at profound economic cost. Understanding the properties of neural disturbances in SCZ constitutes an important research goal, to identify pathophysiological mechanisms and advance biomarker development. Given noted hypotheses for brain-wide disturbances in cortical and subcortical computations (13), we hypothesized that SCZ might be associated with GS alterations. However, most rs-fcMRI studies discard the GS to better isolate functional networks. Such removal may fundamentally obscure meaningful brain-wide GS alterations in SCZ. It is currently unknown whether prevalent implementation of such methods affects our understanding of BOLD signal abnormalities in SCZ or other clinical conditions that share many risk genes, such as bipolar disorder (BD) (14).

Spontaneous BOLD signal can exhibit coherence both within discrete brain networks and over the entire brain (7). In neuroimaging, signal averaged across all voxels is defined as GS. The GS can to a large extent reflect nonneuronal noise (e.g., physiological, movement, scanner-related) (9), which can induce artifactual high correlations across the brain. Thus, GS is often removed via global signal regression (GSR) to better isolate functional networks. This analytic step presumes that brain-wide GS is not of interest, and its removal can improve the anatomical specificity of some rs-fcMRI findings (15). However, this common approach remains controversial (16). Besides noise, GS may reflect neurobiologically important information (7) that is possibly altered in clinical conditions. This reflection is potentially problematic when comparing rs-fcMRI between diagnostic groups that may have different GS profiles. Thus, GS removal may discard critical discriminative information in such instances. This possibility has received little attention in rs-fcMRI studies of severe neuropsychiatric disease, such as SCZ.

We systematically characterized the GS profile across two large and independent SCZ samples ($n = 90$ and $n = 71$), where the first "discovery" sample established novel results and the second sample replicated all effects. To establish diagnostic specificity of SCZ findings, we compared them to a cohort of BD patients ($n = 73$). As a secondary objective, we examined if GSR alters inferences across clinical groups in empirical data. We used both data-driven (17) and seed-based analyses (6, 18)

Significance

This study identified elevated global brain signal variability in schizophrenia, but not bipolar illness. This variability was related to schizophrenia symptoms. A commonly used analytic procedure in neuroimaging, global signal regression, attenuated clinical effects and altered inferences. Furthermore, local voxel-wise variance was increased in schizophrenia, independent of global signal regression. Finally, neurobiologically grounded computational modeling suggests a putative mechanism, whereby altered overall connection strength in schizophrenia may underlie observed empirical results.

Author contributions: G.J.Y., J.D.M., G.R., M.W.C., C.P., J.H.K., G.D.P., D.C.G., and A.A. designed research; G.J.Y., J.D.M., G.R., M.W.C., A.S., M.F.G., G.D.P., D.C.G., and A.A. performed research; G.J.Y., J.D.M., G.R., M.W.C., X.-J.W., and A.A. contributed new reagents/analytic tools; G.J.Y., J.D.M., G.R., M.W.C., A.S., and A.A. analyzed data; and G.J.Y., J.D.M., C.P., and A.A. wrote the paper.

Conflict of interest statement: J.H.K. consults for several pharmaceutical and biotechnology companies with compensation less than $10,000 per year.

This article is a PNAS Direct Submission.

[1]G.J.Y. and J.D.M. contributed equally to this work.

[2]To whom correspondence should be addressed. E-mail: alan.anticevic@yale.edu.

This article contains supporting information online at www.pnas.org/lookup/suppl/doi:10.1073/pnas.1405289111/-/DCSupplemental.

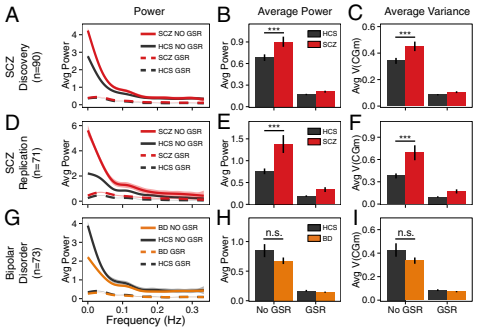

Fig. 1. Power and variance of CGm signal in SCZ and BD. (*A*) Power of CGm signal in 90 SCZ patients (red) relative to 90 HCS (black) (see *SI Appendix*, Table S1 for demographics). (*B*) Mean power across all frequencies before and after GSR indicating an increase in SCZ [$F(1, 178) = 7.42$, $P < 0.01$], and attenuation by GSR [$F(1, 178) = 5.37$, $P < 0.025$]. (*C*) CGm variance also showed increases in SCZ [$F(1, 178) = 7.25$, $P < 0.01$] and GSR-induced reduction in SCZ [$F(1, 178) = 5.25$, $P < 0.025$]. (*D–F*) Independent SCZ sample (see *SI Appendix*, Table S2 for demographics), confirming increased CGm power [$F(1, 143) = 9.2$, $P < 0.01$] and variance [$F(1, 143) = 9.25$, $P < 0.01$] effects, but also the attenuating impact of GSR on power [$F(1, 143) = 7.75$, $P < 0.01$] and variance [$F(1, 143) = 8.1$, $P < 0.01$]. (*G–I*) Results for BD patients ($n = 73$) relative to matched HCS (see *SI Appendix*, Table S3 for demographics) did not reveal GSR effects observed in SCZ samples [$F(1, 127) = 2.89$, $P = 0.092$, n.s.] and no evidence for increase in CGm power or variance. All effects remained when examining all gray matter voxels (*SI Appendix*, Fig. S1). Error bars mark ± 1 SEM. ***$P < 0.001$ level of significance. n.s., not significant.

focused on prefrontal and thalamo-cortical circuits, where dysconnectivity in SCZ has been well established. Finally, we used biologically informed computational modeling (19, 20) to explore how alterations in local circuit parameters could impact emergent GS alterations, as observed in SCZ.

Collectively, results illustrate that GS is differentially altered in neuropsychiatric conditions and may contain neurobiologically meaningful information suggesting that GS should be explicitly analyzed in clinical studies. Our modeling simulations reveal that net increases in microcircuit coupling or global connectivity may underlie GS alterations in SCZ.

Results

Power and Variance of the Cortical Gray Matter BOLD Signal Is Increased in SCZ. We examined the cortical gray matter (CGm) BOLD signal power spectrum in SCZ patients ($n = 90$), compared with matched healthy comparison subjects (HCS, $n = 90$) (6). Using the multitaper periodogram method (21) (*SI Appendix*), we compared the group-averaged power across frequencies, with and without GSR (Fig. 1). To perform GSR, the average signal over all voxels in the brain (GS) was included as a nuisance predictor and regressed out to produce a residual BOLD signal without its GS component (*SI Appendix*). SCZ patients exhibited higher CGm average power [$F(1, 178) = 7.42$, $P < 0.01$] and variance [$F(1, 178) = 7.24$, $P < 0.01$] than HCS (i.e., *Group* main effect). As expected, removal of GS (and its frequency contributions) through GSR reduced the power amplitudes in all frequency domains across groups [$F(1, 178) = 248.31$, $P < 0.0001$]) and attenuated CGm variance [$F(1, 178) = 245.6$, $P < 0.0001$] (i.e., main effect of *Preprocessing*). SCZ patients showed greater reductions in CGm power (averaged over all subjects and frequency domains) [$F(1, 178) = 5.37$, $P < 0.025$] and variance [$F(1, 178) = 5.25$, $P < 0.025$] because of GSR (i.e., *Group* × *Preprocessing* interaction) (Fig. 1 *A–C*). Put simply, the GSR effect was greater in SCZ than HCS. To verify "discovery" findings, we repeated analyses in an independent sample of 71 SCZ patients and 74 HCS, fully replicating increased CGm power/variance in SCZ and the effect of GSR (Fig. 1 *D–F*). Reported effects held when examining all gray matter tissue (as opposed to cortex only) (*SI Appendix*, Fig. S1) and were not present in ventricles (*SI Appendix*, Fig. S2). Interestingly, SCZ effects were more preferential for higher-order networks, but were not evident in visual/motor networks (*SI Appendix*, Fig. S12), suggesting that, despite robust GS effects, elevated variability may be particularly apparent in associative networks. We also controlled for known confounds (movement, smoking, medication dose and medication type), which did not explain reported findings (*Discussion* and *SI Appendix*, Figs. S3 and S14).

Next, to investigate the diagnostic specificity of SCZ effects, we examined an independent sample of 73 BD patients and 56 matched HCS. Strikingly, there was no increase in CGm power in BD relative to HCS; the trend was toward reduced CGm power in BD, the opposite of what we observed in SCZ [$F(1, 127) = 3.06$, $P = 0.083$, n.s.]. GSR did not significantly alter the between-group difference for BD vs. HCS [no *Group* × *Preprocessing* interaction: $F(1, 127) = 2.9$, $P = 0.092$, n.s.] (Fig. 1 *G–I*). In addition, SCZ effects remained relative to BD patients after explicit movement matching (*SI Appendix*, Fig. S12) and controlling for medication type (*SI Appendix*, Fig. S14).

Finally, to establish the clinical relevance of SCZ effects, we examined the relationship of CGm power and variance with SCZ symptom severity (Fig. 2 and *SI Appendix*, Fig. S4). In the discovery sample ($n = 90$), we identified a significant relationship between positive SCZ symptoms and the magnitude of average CGm power before GSR ($r = 0.18$, $P < 0.03$; $\rho = 0.2$, $P < 0.015$). Effects replicated in the independent SCZ cohort [$r = 0.18$, $P < 0.05$; $\rho = 0.18$, $P < 0.05$; joint P (independent replications) < 0.002] (Fig. 2) and were particularly prominent for *Disorganization* symptoms across samples [ρ(discovery) $= 0.26$, $P < 0.01$; ρ(replication) $= 0.25$, $P < 0.025$; joint P (independent replications) < 0.001]. Interestingly, symptom effects were attenuated and no longer significant following GSR, suggesting removal of clinically meaningful information.

Elevated Voxel-Wise Variance in SCZ Remains Following GSR. We demonstrated that SCZ is associated with elevated power/variance relative to HCS both across cortex and all gray matter (Fig. 1 and *SI Appendix*, Fig. S1). It remains unknown if SCZ is associated with altered "local" variance structure of each voxel's time series. To test this hypothesis, we compared whole-brain voxel-wise variance maps across diagnostic groups (Fig. 3). If specific regions are driving the increases in CGm power/variance, this analysis should reveal focal (or region-specific) clusters of between-group difference.

We identified increased voxel-wise variance in SCZ relative to HCS, across discovery and replication samples (Fig. 3*A*). At first, the increase appeared diffuse, suggesting widespread increases in voxel-wise signal variance in SCZ. We tested for preferential

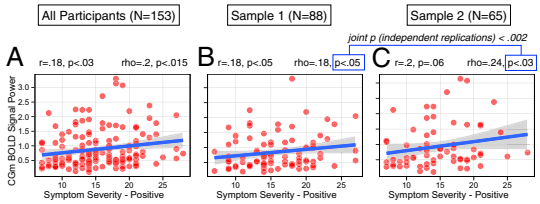

Fig. 2. Relationship between SCZ symptoms and CGm BOLD signal power. We extracted average CGm power for each patient with available symptom ratings ($n = 153$). (*A*) Significant positive relationship between CGm power and symptom ratings in SCZ ($r = 0.18$, $P < 0.03$), verified using Spearman's ρ given somewhat nonnormally distributed data ($\rho = 0.2$, $P < 0.015$). (*B* and *C*) Results held across SCZ samples, increasing confidence in the effect (i.e., joint probability of independent effects $P < 0.002$, marked in blue boxes). All identified relationships held when examining Gm variance (*SI Appendix*, Fig. S4). Notably, all effects were no longer significant after GSR, suggesting GS carries clinically meaningful information. The shaded area marks the 95% confidence interval around the best-fit line.

colocalization of voxel-wise effects, again showing robust effects within the fronto-parietal control network (*SI Appendix*, Fig. S13). The spatial pattern remained virtually unchanged after GSR, indicating that increased BOLD variance in SCZ has both local and global components that are at least somewhat independent of one another. Of note, local variance effects were somewhat apparent across tissues (*SI Appendix*, Fig. S5).

These patterns of increased voxel-wise variance were again specific to SCZ (Fig. 3*B*): BD patients showed no such increase before or after GSR. Importantly, these results were also fully movement scrubbed, reducing the possibility that the increased voxel-wise variance in SCZ was exclusively driven by motion (22) (however, see *Discussion*). These findings illustrate the need to carefully decompose signal variance into global and local components, which may be differentially affected in neuropsychiatric conditions (see modeling for possible neurobiological implications).

Data-Driven Prefrontal Connectivity Results Are Altered Because of Higher GS Variance in SCZ. Present effects have important implications for the widespread use of GSR in rs-fcMRI clinical studies, which remains controversial (16, 23). If groups differ in GS properties, GSR may affect between-group differences in complex ways (23). Informed by the neurobiology of SCZ, we tested this possibility in two ways: focusing on prefrontal cortex (PFC) (17) and thalamo-cortical networks (6, 18, 24).

It is well established that SCZ involves profound alterations in PFC networks (25). Previous rs-fcMRI studies have identified specific functional connectivity reductions in the lateral PFC in chronic SCZ patients (17). Using a data-driven global brain connectivity (GBC) analysis restricted to the PFC (rGBC), we tested whether GSR affects this pattern of between-group differences (*SI Appendix*). Here we collapsed the two SCZ samples to achieve maximal statistical power (n = 161). With GSR, we replicated prior findings (17) showing reduced lateral PFC rGBC in SCZ (Fig. 4). Without GSR, however, between-group difference patterns were qualitatively altered (Fig.4 *A* and *B*): we found evidence for increased rGBC in chronic SCZ, and no evidence for reductions.

This discrepancy between analyses could have occurred for two reasons. First, because of large GS variance in SCZ, GSR could have resulted in a "uniform" transformation of variance structure, whereby the mean between-group difference is reduced but the topography of voxel-wise between-group differences remains the same (Fig. 4*E*). Despite the unchanged topography of the between-group difference, statistical thresholding may lead to qualitatively distinct between-group inferences after GSR in this scenario (Fig. 4*E*). Alternatively, GSR could alter the topography of rGBC differentially across groups, resulting in qualitatively different results before and after GSR (i.e., a non-uniform transformation) (Fig. 4*F*). It is vital to distinguish between these two alternatives in patient data because of complex implications the second possibility may have on clinical resting-state studies (16).

To this end, we computed a quantitative index of statistical similarity (eta^2) for the PFC rGBC between-group difference maps before and after GSR using validated metrics (26). If GSR fundamentally altered the topography of rGBC, we would expect low similarity. However, we found high similarity in the structure of rGBC computed with and without GSR (*SI Appendix*, Fig. S8), suggesting a relatively uniform transform of the between-group effect after GSR (Fig. 4*E*).

Further analysis of the thalamo-cortical connectivity also suggests preserved structure of between-group inferences following GSR (*SI Appendix*, Figs. S6 and S7), replicating prior studies (18). However, GSR shifted the distributions of thalamo-cortical connectivity for all groups into the negative range (*SI Appendix*, Figs. S6 and S7), impacting some conclusions drawn from the data (*Discussion* and *SI Appendix*).

Collectively, these results do not definitively answer whether to use GSR in clinical connectivity studies. Instead, effects suggest that GS needs to be characterized explicitly in clinical groups to determine its contributions in connectivity analyses (*SI Appendix*, Figs. S6 and S7). Based on the outcome of such analyses, researchers can reach a more informed decision if GSR is advisable for specific analyses (*Discussion*).

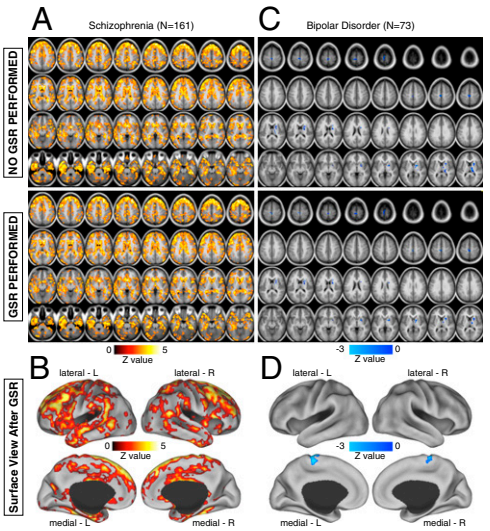

Fig. 3. Voxel-wise variance differs in SCZ independently of GS effects. Removing GS via GSR may alter within-voxel variance for SCZ. Given similar effects, we pooled SCZ samples to maximize power (n = 161). (*A* and *B*) Voxel-wise between-group differences; yellow-orange voxels indicate greater variability for SCZ relative to HCS (whole-brain multiple comparison protected; see *SI Appendix*), also evident after GSR. These data are movement-scrubbed reducing the likelihood that effects were movement-driven. (*C* and *D*) Effects were absent in BD relative to matched HCS, suggesting that local voxel-wise variance is preferentially increased in SCZ irrespective of GSR. Of note, SCZ effects were colocalized with higher-order control networks (*SI Appendix*, Fig. S13).

Understanding Global Signal and Local Variance Alterations via Computational Modeling. Presented results reveal two key observations with respect to variance: (*i*) increased whole-brain voxel-wise variance in SCZ, and (*ii*) increased GS variance in SCZ. The second observation suggests that increased CGm (and Gm) power and variance (Fig. 1 and *SI Appendix*, Fig. S1) in SCZ reflects increased variability in the GS component. This finding is supported by the attenuation of SCZ effects after GSR. To explore potential neurobiological mechanisms underlying such increases, we used a validated, parsimonious, biophysically based computational model of resting-state fluctuations in multiple parcellated brain regions (19). This model generates simulated BOLD signals for each of its nodes (n = 66) (Fig. 5*A*). Nodes are simulated by mean-field dynamics (20), coupled through structured long-range projections derived from diffusion-weighted imaging in humans (27). Two key model parameters are the strength of local, recurrent self-coupling (w) within nodes, and the strength of long-range, "global" coupling (G) between nodes (Fig. 5*A*). Of note, G and w are effective parameters that describe the net contribution of excitatory and inhibitory coupling at the circuit level (20) (see *SI Appendix* for details). The pattern of functional connectivity in the model best matches human patterns when the values of w and G set the model in a regime near the edge of instability (19). However, GS and local variance properties derived from the model had not been examined previously, nor related to clinical observations. Furthermore, effects of GSR have not been tested in this model.

Therefore, we computed the variance of the simulated local BOLD signals of nodes (local node-wise variability) (Fig. 5 *B* and *C*), and the variance of the "global signal" computed as the spatial average of BOLD signals from all 66 nodes (global model

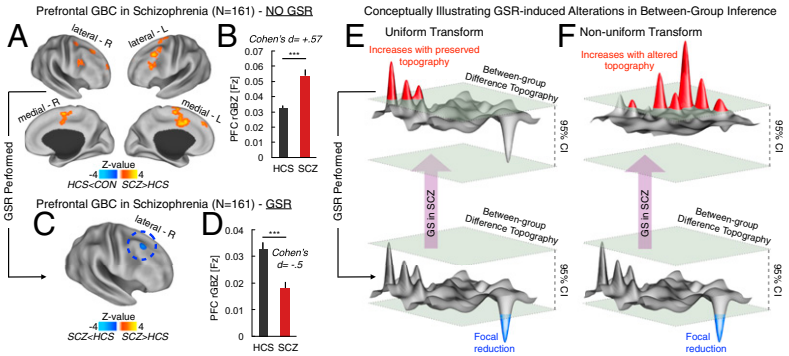

Fig. 4. rGBC results qualitatively change when removing a large GS component. We tested if removing a larger GS from one of the groups, as is typically done in connectivity studies, alters between-group inferences. We computed rGBC focused on PFC, as done previously (17), before (*A* and *B*) and after GSR (*C* and *D*). Red-yellow foci mark increased PFC rGBC in SCZ, whereas blue foci mark reductions in SCZ relative to HCS. Bars graphs highlight effects with standard between-group effect size estimates. Error bars mark ± 1 SEM. (*E*) GSR could uniformly/rigidly transform between-group difference maps. Because of larger GS variability in SCZ (purple arrow) the pattern of between-group differences is shifted, rendering increased connectivity in SCZ as the dominant profile (red signal above the 95% confidence interval indicated by green planes). If GSR shifts the distribution uniformly, then the increased connectivity is now within the 95% confidence interval, but focal reduction becomes apparent with preserved topography. (*F*) Alternatively, GSR could differentially impact the spatial pattern (i.e., nonuniformly transforming data, illustrated by a qualitatively different pattern before and after GSR). We conducted focused analyses to arbitrate between these possibilities, suggesting that the effect is predominantly uniform (*SI Appendix*, Fig. S8). Note: topographies in *E* and *F* represent a conceptual illustration, and do not reflect specific patient data. ***$P < .001$.

variability) (Fig. 5 *D* and *E*). Critically, this in silico global signal differs from empirical GS because it contains only neural contributions (and by definition no physiological artifact). We examined model dynamics as a function of w and G (see parameter space in Fig. 5*F*). The local variance of each node increased as a function of increasing w and G (Fig. 5 *B* and *C*). This finding suggests that the empirically observed increase in voxel-wise variance in SCZ might arise from increased neural coupling at the local and long-range scales. The variance of simulated GS increased as a function of increasing w and G (Fig. 5 *D* and *E*). These effects were robust to particular patterns of large-scale anatomical connectivity (*SI Appendix*, Fig. S9). Finally, effects of GSR resulted in attenuated model-based variance, a pattern that was quite similar to clinical effects (Fig. 5 *B*–*E*, dashed lines; see *SI Appendix* for GSR implementation). The GS variance was completely attenuated given that in silico GSR effectively removes the model-derived signal mean across all time points.

These modeling findings illustrate that GS and local variance alterations can possibly have neural bases (as opposed to driven exclusively by physiological or movement-induced artifacts). The abnormal variance in SCZ could arise from changes in w and G, perhaps leading to a cortical network that operates closer to the edge of instability than in HCS (Fig. 5*F*).

Discussion

Power and Variability of BOLD Signals in SCZ. Local cortical computations, and in turn large-scale neural connectivity, are profoundly altered in SCZ (13). One outcome of such dysconnectivity could be an alteration in the distributed gray matter BOLD signal, reflected in increased variance/power. We identified results consistent with this hypothesis before GSR in a large SCZ sample ($n = 90$), and replicated findings in an independent sample ($n = 71$). This effect was absent in BD patients, supporting diagnostic specificity of SCZ effects. After GSR, the BOLD signal power/variance for cortex and gray matter was significantly reduced across SCZ samples, consistent with GSR removing a large variance from the BOLD signal (28). However, removing a GS component that contributes abnormally large BOLD signal variance in SCZ could potentially discard clinically important information arising from the neurobiology of the disease, as suggested by symptom analyses. Such increases in GS variability may reflect abnormalities in underlying neuronal activity in SCZ. This hypothesis is supported by primate studies showing that resting-state fluctuations in local field potential at single cortical sites are associated with distributed signals that correlate positively with GS (7). Furthermore, maximal GSR effects colocalized in higher-order associative networks, namely the fronto-parietal control and default-mode networks (*SI Appendix*, Fig. S12), suggesting that abnormal BOLD signal variance increases may be preferential for associative cortices that are typically implicated in SCZ (29, 30).

Although it is difficult to causally prove a neurobiological source of increased GS variance here (given the inherent correlational nature of BOLD effects), certain analyses add confidence for such an interpretation. First, the effect was not related to smoking or medication. Second, the effect survived in movement-scrubbed and movement-matched data, inconsistent with head-motion being the dominant factor. Third, albeit modest in magnitude, increased CGm power was significantly related to SCZ symptoms (particularly before GSR), an effect that

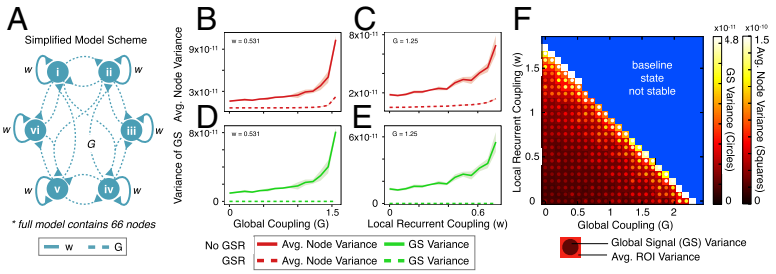

Fig. 5. Computational modeling simulation of BOLD signal variance illustrates a biologically grounded hypothetical mechanism for increased global and local variance. (*A*) We used a biophysically based computational model of resting-state BOLD signals to explore parameters that could reflect empirical observations in SCZ. The two key parameters are the strength of local, recurrent self-coupling (w) within nodes (solid lines), and the strength of long-range, global coupling (G) between 66 nodes in total (dashed lines), adapted from prior work (19) (*B* and *C*) Simulations indicate increased variance of local BOLD signals originating from each node, in response to increased w or G. (*D* and *E*) The GS, computed as the spatial average across all nodes, also showed increased variance by elevating w or G. Shading represents the SD at each value of w or G computed across four realizations with different starting noise, illustrating model stability. Dotted lines indicate effects after in silico GSR. (*F*) Two-dimensional parameter space, capturing the positive relationship between w/G and variance of the BOLD signal at the local node level (squares, far right color bar) and the GS level (circles in each square, the adjacent color bar). The blue area marks regimes where the model baseline is associated with unrealistically elevated firing rates of simulated neurons. Model simulations illustrate how alterations in biophysically based parameters (rather than physiological noise) can increase GS and local variance observed empirically in SCZ. Of note in *B*–*E*, when w is modulated, $G = 1.25$. Conversely, when G is modulated, $w = 0.531$. For permutations of anatomical connectivity matrixes, mean trends and complete GSR effects, see *SI Appendix*, Figs. S9–S11.

replicated across samples, thus unlikely to have occurred by chance alone. Importantly, CGm/Gm power and variance increases were diagnostically specific, as the pattern was not identified in BD patients, even when controlling for movement and medication type (*SI Appendix*, Figs. S3 and S14). Of note, cumulative medication impact is notoriously difficult to fully capture quantitatively in cross-sectional studies of chronic patients; therefore, longitudinal study designs are needed to confirm present effects (although, see *SI Appendix*, Fig. S14). Finally, given evidence for network specificity of present SCZ effects, it is highly unlikely that metabolic, cardiovascular, movement or breathing-rate effects impacted these results (i.e., effects were not as evident in sensory-motor and visual networks, although present in associative networks) (*SI Appendix*, Fig. S12). Nevertheless vigilance levels (31) need to be ruled out (32).

Importantly, findings are indicative of a coherent signal contribution as opposed to random noise (supported by power analysis). Increased power could indicate disrupted neuronal communication, reflecting a shift in the baseline amplitude or durations of cortex-wide signals. A global increase in durations of signal oscillations across frequencies, revealed in increased average power, could reflect globally delayed inhibition of local microcircuit signals in the setting of altered global connectivity.

In addition to elevated GS variance, we examined local voxel-wise variance in SCZ. We observed, irrespective of GSR, that SCZ is associated with increased local voxel-wise variance. The effect was again diagnostically specific and not found in BD, highlighting three points: (*i*) The unchanged whole-brain voxel-wise variance pattern illustrates that the spatial distribution of this variability is largely unaffected by GSR. (*ii*) Even when high-variance GS is removed, there remains greater voxel-wise variability in SCZ (despite movement-scrubbing). (*iii*) Interestingly, both the GS and voxel-wise effects colocalized preferentially around associative cortices (*SI Appendix*, Figs. S12 and S13), suggesting that these disturbances may reflect signal alterations in specific higher-order control networks, in line with recent connectivity findings (30).

Although these analyses were performed on movement-scrubbed data, it may be possible that micromovements still remain (33), which studies using faster acquisition (34) could address. Relatedly, a recent rigorous movement-related investigation (35) suggests that motion artifacts can spatially propagate as complex waveforms in the BOLD signal across multiple frames.

Effect of Large GS Variance on Between-Group Comparisons: Methodological Implications. A key objective of this study was empirical, namely to establish evidence for greater GS variance in SCZ. However, this finding has methodological implications for many future clinical connectivity studies, as GSR has been hypothesized to impact patterns of between-group differences in such studies (16, 23). Here it is important to examine which measures may be sensitive to GSR in between-group clinical comparisons because of greater GS variance in SCZ. We tested this using two broad approaches centered on system-level abnormalities implicated in SCZ, namely thalamo-cortical (24) and PFC dysconnectivity (17, 36).

Across all thalamo-cortical analyses we found that, irrespective of GSR, SCZ was associated with the same relative direction of differences compared with HCS, as reported previously (18). However, an interesting motif emerged: before GSR the direction of the effect suggested that SCZ and HCS display positive thalamo-cortical connectivity, wherein the magnitude of SCZ connections exceed those of HCS. In contrast, after GSR both groups were associated with negative thalamo-cortical connectivity, wherein the magnitude of SCZ was lesser than HCS. Here we also considered using correlations versus covariance to quantify thalamo-cortical signals, given arguments suggesting that correlation coefficients may not be always ideal (37) (*SI Appendix*, Figs. S6 and S7). These results highlight that clinical studies dealing with different magnitudes of BOLD signal variance across groups may consider decomposing correlations, to allow a nuanced inference regarding the alterations in functional connectivity.

We also tested if GSR impacts data-driven patterns of between-group differences. We used a well-validated data-driven metric to capture global PFC connectivity (17). In contrast to thalamo-cortical results, GSR affected between-group rGBC inferences. Using GSR we replicated prior findings indicating reductions in rGBC centered on lateral PFC (17). However, without GSR the pattern of between-group differences was consistent with PFC hyperconnectivity in chronic SCZ, in contrast to prevalent hypotheses that postulate PFC hypofunction (25). This discrepancy raises an important point: significant differences in rGBC results pre- and post-GSR show that GSR can affect some between-group inferences.

The discrepancy, however, could have occurred because of two very different scenarios, which have distinct implications regarding GSR effects on between-group comparisons. One possibility, suggested by certain mathematical modeling simulations (16), is a nonuniform data transformation when removing a larger GS from one group. Furthermore, if the magnitude of the global BOLD variability is larger for one group, in combination with this nonuniform effect, then the resulting between-group effect will be different in magnitude and spatial pattern (Fig. 4*F*). The alternative is that GSR generally induces a rigid or uniform data transformation (Fig. 4*E*). Put differently, the magnitude of the total Gm variability may be greater for one group, but its spatial effect on voxel-wise connectivity is the same across groups. Present findings support the latter possibility (*SI Appendix*, Fig. S8), suggesting that GS removal does not fundamentally alter the spatial topography of between-group differences.

Collectively, PFC and thalamic analyses indicate that GSR does not necessarily always change between-group inferences. In cases where GSR qualitatively altered between-group effects, the discrepancy reflected a uniform data shift (Fig. 4). Nevertheless, removing a GS component from one group could affect the conclusions drawn about some between-group difference (given the observed sign reversal) (28). Therefore, the preferred strategy for future clinical connectivity studies may be twofold: (*i*) studies should first carefully examine GS magnitude and power spectra in each group to determine if they are indeed different; and (*ii*) studies should test for the direction of clinical inferences before and after GSR to allow a nuanced interpretation regarding the observed connectivity alterations (16). Such a stepwise approach is critical to circumvent the debate whether to use GSR or not and instead use rigorous data inspection to support appropriate study-specific analytic decisions (see *SI Appendix* for further discussion).

Neurobiological Mechanisms of GS Alterations in SCZ. Lastly, we studied a biophysically based computational model of rs-fcMRI to enhance our understanding of BOLD effects in SCZ (19). The simulations showed increased GS variance after elevating local node self-coupling (w) and global coupling (G) between nodes. The modeling results also revealed a collective increase in local variance for all simulated nodes as a result of increasing w or G parameters. These simulations serve as an initial proof-of-principle, showing that changes in GS and local variance can have neural bases, rather than purely reflecting nonneural variables (as the model explicitly excludes such signal sources). Empirical measures of local and GS variability can potentially be used to probe specific neurobiological changes in cortical microcircuitry and long-range interactions. Applying this model to healthy humans, Deco et al. proposed that resting-state cortex operates near the edge of instability, based on matching the empirically observed functional connectivity (19). Using a similar architecture, we show that GS and local variance increase near the edge of the instability by elevating w and G. It is possible that SCZ patients operate even closer to this edge than in HCS, which could potentially expose a vulnerability to perturbations. Furthermore, in silico GSR attenuated this increase in variance, as observed clinically (dashed lines in Figs. 1 and 5). Future studies can extend these proof-of-principle modeling findings to interpret BOLD signal changes following SCZ illness progression (13), which would also better control for some limitations of present

cross-section data. In turn, modeling can provide insights for neuroimaging studies using pharmacological interventions, such as the NMDA receptor antagonist ketamine, which may alter local and long-range synaptic interactions in vivo (38).

Of note, SCZ is associated with both glutamatergic (excitatory) and GABAergic (inhibitory) deficits in local microcircuits (39) as well as striatal dopamine abnormalities (40). Within the model, G and w reflect the net contributions of excitatory and inhibitory interactions in cortical circuits. Other computational modeling and neurophysiological evidence using behaving monkeys (41) suggest that a reduction of local recurrent excitation could explain cognitive deficits associated with SCZ. Present results can be reconciled with these observations by considering excitation/inhibition balance (E/I balance) (42). Our modeling results suggest that in the resting state, SCZ is associated with an increased E/I balance of either local or long-range, which is in line with the hypothesis of prominent inhibitory deficits in chronic SCZ (43). It remains to be determined how current modeling simulations relate to complex network measures (36) and to task-based cognitive deficits observed in SCZ (44).

Conclusion

This study addresses vital gaps in understanding GS in neuropsychiatric illness. (*i*) Results show that the GS is profoundly altered in SCZ but not BD. (*ii*) GSR can affect between-group analyses, altering conclusions in complex ways. (*iii*) Results show that future clinical neuroimaging studies need to systematically assess GS and consider its impact upon system-level connectivity inferences. Finally, this study highlights the possible neurobiological importance of global/local BOLD signal variance alterations in SCZ, which may relate to synaptic coupling disruptions that could be amenable to pharmacological intervention.

Experimental Procedures

Participants. For comprehensive procedures regarding subject selection, inclusion/exclusion criteria, group matching, medication, and symptom analyses, see *SI Appendix*.

Neuroimaging. For a full description of acquisition, processing and all neuroimaging analyses see *SI Appendix*.

Computational Modeling. We used a validated computational model of resting-state functional connectivity (19), extending a local circuit model (20) to incorporate biologically plausible mechanisms for BOLD signal fluctuations. Complete modeling details are presented in the *SI Appendix*.

ACKNOWLEDGMENTS. We thank Dr. David Van Essen for helpful comments during manuscript preparation; Dr. Francis Song for assistance with implementing anatomical connectivity into the model; and Dr. Vince Calhoun for assistance with the publicly available Center for Biomedical Research Excellence dataset. Financial support was provided by National Institutes of Health Grants DP50D012109-02 [to A.A., PI (principal investigator)], MH080912 (to D.C.G., PI), MH096801 (to M.W.C., PI), and MH43775, MH077945, and MH074797 (to G.D.P., PI); National Institute on Alcohol Abuse and Alcoholism Grant 2P50AA012870-11 (to J.H.K., PI); the Fulbright Foundation (A.S.); the National Alliance for Research on Schizophrenia and Depression Young Investigator Award (to A.A., PI); Grant R01-MH062349 (to J.D.M. and X.-J.W.); and National Institutes of Health Grant T32GM 007205 (to G.J.Y.).

1. Biswal BB, et al. (2010) Toward discovery science of human brain function. *Proc Natl Acad Sci USA* 107(10):4734–4739.
2. Fox MD, et al. (2005) The human brain is intrinsically organized into dynamic, anticorrelated functional networks. *Proc Natl Acad Sci USA* 102(27):9673–9678.
3. Buckner RL, Krienen FM, Yeo BT (2013) Opportunities and limitations of intrinsic functional connectivity MRI. *Nat Neurosci* 16(7):832–837.
4. Smith SM, et al. (2009) Correspondence of the brain's functional architecture during activation and rest. *Proc Natl Acad Sci USA* 106(31):13040–13045.
5. Fox MD, Greicius M (2010) Clinical applications of resting state functional connectivity. *Front Syst Neurosci* 4:19.
6. Anticevic A, et al. (2013) Characterizing thalamo-cortical disturbances in schizophrenia and bipolar illness. *Cereb Cortex*, 10.1093/cercor/bht165.
7. Schölvinck ML, Maier A, Ye FQ, Duyn JH, Leopold DA (2010) Neural basis of global resting-state fMRI activity. *Proc Natl Acad Sci USA* 107(22):10238–10243.
8. Stephan KE, Baldeweg T, Friston KJ (2006) Synaptic plasticity and dysconnection in schizophrenia. *Biol Psychiatry* 59(10):929–939.
9. Coyle JT (2006) Glutamate and schizophrenia: Beyond the dopamine hypothesis. *Cell Mol Neurobiol* 26(4-6):365–384.
10. Marín O (2012) Interneuron dysfunction in psychiatric disorders. *Nat Rev Neurosci* 13(2):107–120.
11. Walker E, Kestler L, Bollini A, Hochman KM (2004) Schizophrenia: Etiology and course. *Annu Rev Psychol* 55:401–430.
12. Murray CJL, Lopez AD (1996) *The Global Burden of Disease: A Comprehensive Assessment of Mortality and Disability from Diseases, Injuries and Risk Factors in 1990 and Projected to 2020* (Harvard Univ Press, Cambridge, MA).
13. Uhlhaas PJ (2013) Dysconnectivity, large-scale networks and neuronal dynamics in schizophrenia. *Curr Opin Neurobiol* 23(2):283–290.
14. Khadka S, et al. (2013) Is aberrant functional connectivity a psychosis endophenotype? A resting state functional magnetic resonance imaging study. *Biol Psychiatry* 74(6):458–466.
15. Fox MD, Zhang D, Snyder AZ, Raichle ME (2009) The global signal and observed anticorrelated resting state brain networks. *J Neurophysiol* 101(6):3270–3283.
16. Saad ZS, et al. (2012) Trouble at rest: How correlation patterns and group differences become distorted after global signal regression. *Brain Connect* 2(1):25–32.
17. Cole MW, Anticevic A, Repovs G, Barch DM (2011) Variable global dysconnectivity and individual differences in schizophrenia. *Biol Psychiatry* 70(1):43–50.
18. Woodward ND, Karbasforoushan H, Heckers S (2012) Thalamocortical dysconnectivity in schizophrenia. *Am J Psychiatry* 169(10):1092–1099.
19. Deco G, et al. (2013) Resting-state functional connectivity emerges from structurally and dynamically shaped slow linear fluctuations. *J Neurosci* 33(27):11239–11252.
20. Wong KF, Wang XJ (2006) A recurrent network mechanism of time integration in perceptual decisions. *J Neurosci* 26(4):1314–1328.
21. Mitra PP, Pesaran B (1999) Analysis of dynamic brain imaging data. *Biophys J* 76(2):691–708.
22. Power JD, Barnes KA, Snyder AZ, Schlaggar BL, Petersen SE (2013) Steps toward optimizing motion artifact removal in functional connectivity MRI; a reply to Carp. *Neuroimage* 76:439–441.
23. Gotts SJ, et al. (2013) The perils of global signal regression for group comparisons: A case study of autism spectrum disorders. *Front Hum Neurosci* 7:356.
24. Andreasen NC (1997) The role of the thalamus in schizophrenia. *Can J Psychiatry* 42(1):27–33.
25. Goldman-Rakic PS (1991) Prefrontal cortical dysfunction in schizophrenia: The relevance of working memory. *Psychopathology and the Brain*, eds Carroll BJ, Barrett JE (Raven Press, New York), pp 1–23.
26. Cohen AL, et al. (2008) Defining functional areas in individual human brains using resting functional connectivity MRI. *Neuroimage* 41(1):45–57.
27. Hagmann P, et al. (2008) Mapping the structural core of human cerebral cortex. *PLoS Biol* 6(7):e159.
28. Murphy K, Birn RM, Handwerker DA, Jones TB, Bandettini PA (2009) The impact of global signal regression on resting state correlations: Are anti-correlated networks introduced? *Neuroimage* 44(3):893–905.
29. Whitfield-Gabrieli S, et al. (2009) Hyperactivity and hyperconnectivity of the default network in schizophrenia and in first-degree relatives of persons with schizophrenia. *Proc Natl Acad Sci USA* 106(4):1279–1284.
30. Baker JT, et al. (2014) Disruption of cortical association networks in schizophrenia and psychotic bipolar disorder. *JAMA Psychiatry* 71(2):109–118.
31. Wong CW, Olafsson V, Tal O, Liu TT (2013) The amplitude of the resting-state fMRI global signal is related to EEG vigilance measures. *Neuroimage* 83:983–990.
32. Birn RM, Diamond JB, Smith MA, Bandettini PA (2006) Separating respiratory-variation-related fluctuations from neuronal-activity-related fluctuations in fMRI. *Neuroimage* 31(4):1536–1548.
33. Kundu P, et al. (2013) Integrated strategy for improving functional connectivity mapping using multiecho fMRI. *Proc Natl Acad Sci USA* 110(40):16187–16192.
34. Smith SM, et al. (2012) Temporally-independent functional modes of spontaneous brain activity. *Proc Natl Acad Sci USA* 109(8):3131–3136.
35. Power JD, et al. (2014) Methods to detect, characterize, and remove motion artifact in resting state fMRI. *Neuroimage* 84:320–341.
36. Fornito A, Zalesky A, Pantelis C, Bullmore ET (2012) Schizophrenia, neuroimaging and connectomics. *Neuroimage* 62(4):2296–2314.
37. Friston KJ (2011) Functional and effective connectivity: A review. *Brain Connect* 1(1):13–36.
38. Anticevic A, et al. (2012) NMDA receptor function in large-scale anticorrelated neural systems with implications for cognition and schizophrenia. *Proc Natl Acad Sci USA* 109(41):16720–16725.
39. Lewis DA, Hashimoto T, Volk DW (2005) Cortical inhibitory neurons and schizophrenia. *Nat Rev Neurosci* 6(4):312–324.
40. Howes OD, et al. (2012) The nature of dopamine dysfunction in schizophrenia and what this means for treatment. *Arch Gen Psychiatry* 69(8):776–786.
41. Wang M, et al. (2013) NMDA receptors subserve persistent neuronal firing during working memory in dorsolateral prefrontal cortex. *Neuron* 77(4):736–749.
42. Murray JD, et al. (2014) Linking microcircuit dysfunction to cognitive impairment: Effects of disinhibition associated with schizophrenia in a cortical working memory model. *Cereb Cortex* 24(4):859–872.
43. Lewis DA, Curley AA, Glausier JR, Volk DW (2012) Cortical parvalbumin interneurons and cognitive dysfunction in schizophrenia. *Trends Neurosci* 35(1):57–67.
44. Anticevic A, et al. (2012) The role of default network deactivation in cognition and disease. *Trends Cogn Sci* 16(12):584–592.